© 2018. Published by The Company of Biologists Ltd | Journal of Cell Science (2018) 131, jcs213520. doi:10.1242/jcs.213520

RESEARCH ARTICLE

Swe1 and Mih1 regulate mitotic spindle dynamics in budding yeast via Bik1

Erica Raspelli*, Silvia Facchinetti and Roberta Fraschini‡

ABSTRACT

The mitotic spindle is a very dynamic structure that is built *de novo* and destroyed at each round of cell division. In order to perform its fundamental function during chromosome segregation, mitotic spindle dynamics must be tightly coordinated with other cell cycle events. These changes are driven by several protein kinases, phosphatases and microtubule-associated proteins. In budding yeast, the kinase Swe1 and the phosphatase Mih1 act in concert in controlling the phosphorylation state of Cdc28, the catalytic subunit of Cdk1, the major regulator of the cell cycle. In this study we show that Swe1 and Mih1 are also involved in the control of mitotic spindle dynamics. Our data indicate that Swe1 and the Polo-like kinase Cdc5 control the balance between phosphorylated and unphosphorylated forms of Mih1, which is, in turn, important for mitotic spindle elongation. Moreover, we show that the microtubule-associated protein Bik1 is a phosphoprotein, and that Swe1 and Mih1 are both involved in controlling phosphorylation of Bik1. These results uncover new players and provide insights into the complex regulation of mitotic spindle dynamics.

KEY WORDS: Swe1, Mih1, Bik1, Spindle positioning, Phosphorylation, Mitosis, Yeast

INTRODUCTION

During mitosis, the mitotic spindle has the crucial function of accomplishing faithful chromosome segregation between the mother and daughter cell. It comprises microtubules (MTs) that are composed of heterodimers of α- and β-tubulin, which are assembled in a head-to-tail fashion. As a consequence, each MT has a polarity and it has two distinct ends with different properties: a fast-growing plus end and a slowly growing minus end. Spindle structure is highly dynamic during the cell cycle. The spindle has a bipolar nature and is formed by nuclear MTs that originate from two centrosomes, called spindle pole bodies (SPBs) in yeast. In budding yeast, the SPBs are embedded in the nuclear envelope, which does not break down during cell division, so the mitotic spindle is always inside the nucleus. Another class of MTs, the cytoplasmic MTs, emanates from the SPBs towards the cytoplasm: these MTs are essential for interactions between the spindle and the cell cortex, and for spindle movement and orientation (Huffaker et al., 1988).

Università degli Studi di Milano-Bicocca, Dipartimento di Biotecnologie e Bioscienze, Piazza della Scienza 2, 20126 Milano, Italy.
*Present address: IFOM – Istituto FIRC di Oncologia Molecolare, Via Adamello 16, 20139 Milano, Italy.

‡Author for correspondence (roberta.fraschini@unimib.it)

E.R., 0000-0002-0937-0521; S.F., 0000-0001-7771-3904; R.F., 0000-0001-8441-4080

Received 5 December 2017; Accepted 11 July 2018

The budding yeast *Saccharomyces cerevisiae* undergoes an asymmetric cell division. The division site is determined very early during the cell cycle, at the G1/S transition since this is the position of bud emergence that defines where cytokinesis will take place. The bipolar spindle is built during S phase, when the site of cell division is already established, and before anaphase onset it must move towards the bud neck and align along the mother-daughter axis (Piatti et al., 2006). This process is governed by the Kar9 pathway and the Dyn1 pathway. The initial alignment of the spindle requires asymmetric localization of Kar9 to the SPB that will migrate into the bud, the SPB component Nud1/centriolin is involved in this process (Hotz et al., 2012). Then Kar9, in association with the MT binding protein Bim1, is transported to the microtubule plus ends where they interact with the actin-associated myosin Myo2, which then pulls Kar9 and the associated microtubule into the bud (Lee et al., 2000; Fraschini et al., 2008). The second pathway acts during anaphase and it governs the final positioning of the spindle along the cell polarity axis: the motor protein Dyn1, in complex with dynactin, pulls microtubules that are attached to the daughter-bound SPB through the bud neck by association with the cortical protein Num1 (Fraschini et al., 2008; Yeh et al., 1995; Heil-Chapdelaine et al., 2000).

Bik1 is a microtubule-associated protein (MAP), orthologous to human CLIP-170, it localizes at the SPBs and at the plus ends of microtubules and is involved in stabilization of MT length. In particular, Bik1 plays a negative role in MT assembly through inhibition of growth rates, and by enhancing the rate of catastrophes, it produces pulling force on kinetochores before anaphase and is required for spindle elongation during anaphase (Berlin et al., 1990). In addition, Bik1 is involved in mitotic spindle positioning by controlling the recruitment of Dyn1 and Kar9 at the SPBs (Moore et al., 2006). There is a pool of Bik1 localized firmly at the spindle pole body and a soluble pool from which Bik1 can be recruited during microtubule polymerization (Carvalho et al., 2004).

Mitotic spindle dynamics are also controlled by the chromosomal passenger complex (CPC), which consists of Aurora kinase Ipl1, Bir1, Sli15 and Nbl1. The CPC localizes to the kinetochores of chromosomes to regulate their bi-orientation and then it moves to the mitotic spindle during anaphase to control spindle stabilization and elongation (Nakajima et al., 2011; Makrantoni et al., 2014). In late anaphase, the kinase Ipl1 has a dual role in spindle disassembly: it phosphorylates and inactivates Bim1, a MT-plus-end-binding protein (Woodruff et al., 2010; Tirnauer et al., 1999), and phosphorylates and activates the spindle-destabilizing protein She1 (Woodruff et al., 2010). In parallel to Ipl1, MT depolymerization is brought about by Kip3, a kinesin-8 family member that is involved in the regulation of MT length and in spindle movement towards the bud acting in concert with Bim1, Kar9 and Dyn1 (Carvalho et al., 2004, 2003; Pearson et al., 2004).

Journal of Cell Science (2018) 131, jcs213520. doi:10.1242/jcs.213520

Cdc5 is a member of the conserved Polo-like kinase family that consists of many proteins in different species. It is encoded by an essential gene and plays several roles in mitosis and meiosis. Cdc5 is directly involved in MT growth (Park et al., 2008), in SPB separation (Simpson-Lavy et al., 2015), it promotes mitotic exit (Stegmeier et al., 2002) and is involved in Swe1 phosphorylation and inactivation (van de Weerdt and Medema, 2006; Asano et al., 2005).

Swe1 belongs to the Wee-related kinase family; this family has several members, including *Schizosaccharomyces pombe* wee1, *Xenopus* Xwee1 and human WEE1, which are all involved in the control of mitotic entry (Morgan, 1997; Michael and Newport, 1998). In particular, *S. cerevisiae* Swe1 is a tyrosine kinase that inhibits Cdk1 by phosphorylation of Tyr19 in its catalytic subunit, Cdc28 (Booher et al., 1993; Harvey et al., 2005), thus blocking mitosis. This inhibition is important to delay cell cycle progression in response to defects in bud morphogenesis, actin cytoskeleton and septin structure (Lew, 2003). During an unperturbed cell cycle, Swe1 is subjected to multiple regulations that change its phosphorylation state, subcellular localization and protein levels. In particular, during S phase Swe1 accumulates in the nucleus where is it phosphorylated by Clb-Cdc28; in G2 phase, Swe1 is recruited to the mother-bud neck where it undergoes multiple phosphorylation events by different kinases, among which Cdc5 and the PAK (p21-activated kinase) kinase Cla4, that lead to its ubiquitylation and degradation at the G2/M transition (van de Weerdt and Medema, 2006; Asano et al., 2005; Sakchaisri et al., 2004; Howell and Lew, 2012; Raspelli et al., 2011; Longtine et al., 2000). Swe1 degradation is prevented in case of perturbation of the actin or septin cytoskeleton that activate the morphogenesis checkpoint, thereby inhibiting Cdk1 and delaying the cell cycle in G2 (Lew, 2003; Keaton and Lew, 2006; Gladfelter et al., 2005). Besides its major role in the morphogenesis checkpoint, there is some evidence that Swe1 is also involved in other processes. For example, *swe1Δ* mutants are smaller than wild-type cells (Harvey et al., 2003; Jorgensen et al., 2002), so Swe1 may be part of a network that monitors the cell dimension, delaying the cell cycle until the bud has reached a critical size (Kellogg, 2003). Interestingly, *swe1Δ* mutants also exhibit premature spindle elongation (Lianga et al., 2013; Raspelli et al., 2015) and high Swe1 levels block spindle formation, indicating that Swe1 is involved in spindle dynamics (Raspelli et al., 2015). Moreover Swe1 plays a role during filamentous growth (La Valle and Wittenberg, 2001) and, more recently, it has been involved in histone phosphorylation (Mahajan et al., 2012) and SPB inheritance (Lengefeld et al., 2017).

The Swe1-mediated inhibitory phosphorylation of Tyr19 of Cdc28 is reversed by the tyrosine phosphatase Mih1 in order to promote entry into mitosis (Russell et al., 1989). Deletion of Mih1 results in increased cell size, a delay in entry into mitosis (Pal et al., 2008) and spindle elongation (Lianga et al., 2013). Mih1 regulation is complex and not fully understood. Mih1 protein levels are constant during the cell cycle but Mih1 is modified by phosphorylation events, indeed it is hyper-phosphorylated for most of the cell cycle and is dephosphorylated as cells enter mitosis by the protein phosphatase PP2A with its regulatory subunit Cdc55 (Pal et al., 2008). Casein kinase I (CKI) is responsible for most of the hyper-phosphorylation of Mih1 (Pal et al., 2008). Also, Cdk1 appears to directly phosphorylate Mih1, but Cdk1 activity is also required to initiate Mih1 dephosphorylation as cells enter mitosis (Pal et al., 2008). So Mih1 regulation is the result of a balance of kinase and phosphatase activities. In addition, Mih1 is localized throughout the cell during most of the cell cycle and it accumulates in the nucleus during telophase; these dynamics are also important for its function (Keaton et al., 2008).

In this paper, we investigated the role of Swe1 in mitotic spindle regulation further and we show that Swe1 is involved not only in mitotic spindle elongation but also in its positioning. We also show that Swe1 and Cdc5 control Mih1 phosphorylation and activation, which, in turn, controls dephosphorylation of the MAP Bik1 and mitotic spindle elongation. Altogether, our data highlight a new role for Swe1 and Mih1 in mitotic spindle dynamics.

RESULTS

SWE1 deletion affects mitotic spindle positioning

We previously reported that Swe1 is involved in mitotic spindle function independently of its role on Cdc28 phosphorylation (Raspelli et al., 2015). We further investigated this issue by studying the effect of the lack of Swe1 on spindle positioning, a crucial matter for yeast cells, where the site of cell division is determined earlier than bipolar spindle formation. We performed time-lapse analysis of wild-type (wt) and *swe1Δ* cells expressing Tub1-GFP arrested in G1 with α-factor and released in fresh medium. As shown in Fig. 1A,B, we observed that in wt cells, the mitotic spindle is correctly positioned at the bud neck 40.2±4.2 min (mean±s.d.) after release, whereas in *swe1Δ* cells, the same process is slower (53.3±6.2 min). These data indicate that Swe1 is involved in mitotic spindle positioning at the bud neck.

Then, we analysed the effect of the lack of Swe1 on mutants that have altered mitotic spindle dynamics, such as *ipl1-321*, *sli15-3*, *nud1-44*, *kar9Δ*, *bim1Δ*, *kip3Δ*, *dyn1Δ* and *bik1Δ*. We deleted the *SWE1* ORF in the indicated mutant strains and analysed their defect in mitotic spindle positioning after shift to the restrictive temperature for each mutant. Single mutants, double mutants *kar9Δ swe1Δ*, *bim1Δ swe1Δ*, *ipl1-321 swe1Δ*, *sli15-3 swe1Δ*, *nud1-44 swe1Δ* and wild-type cells were grown in rich medium at 25°C and shifted to 37°C. After 3 h, we stained nuclei and counted the presence of two divided nuclei in the mother cell as an index of spindle mispositioning. Wild-type cells showed no defect, whereas *kar9Δ*, *bim1Δ* and *swe1Δ* mutants exhibited small defects, but more importantly, deletion of *SWE1* aggravated the spindle position defect of both mutants, to different extents (Fig. 1C). An additive effect was also evident in *ipl1-321 swe1Δ*, *sli15-3 swe1Δ* and *nud1-44 swe1Δ* double mutants (Fig. 1D). We performed the same analysis in the *swe1Δ kip3Δ* double mutant shifted to 14°C, a restrictive temperature for *kip3Δ* mutant, and we observed that the absence of both Swe1 and Kip3 caused a clear spindle-positioning defects (Fig. 1E). Finally, we analysed *dyn1Δ swe1Δ* and *bik1Δ swe1* double mutants shifted to 14°C: we observed an additive effect on spindle mispositioning in *dyn1Δ swe1Δ* cells, whereas the lack of Swe1 did not exacerbate *bik1Δ* cell defects (Fig. 1F). These data indicate that Swe1 may play a role in mitotic spindle positioning, operating in a different pathway to Ipl1, Sli15, Nud1, Kar9, Bim1 and Dyn1 and acting in concert with the MAP Bik1.

Bik1 is a phosphoprotein

In order to better characterize the role of Swe1 in mitotic spindle dynamics, we decided to gain insight into the interaction between Bik1 and Swe1. Bik1 is a MAP required for spindle elongation (Berlin et al., 1990) and it is involved in mitotic spindle positioning (Moore et al., 2006). However, little is known about its regulation and post-translational modifications. A proteome chip array identified Bik1 as a protein phosphorylated by Swe1

Journal of Cell Science (2018) 131, jcs213520. doi:10.1242/jcs.213520

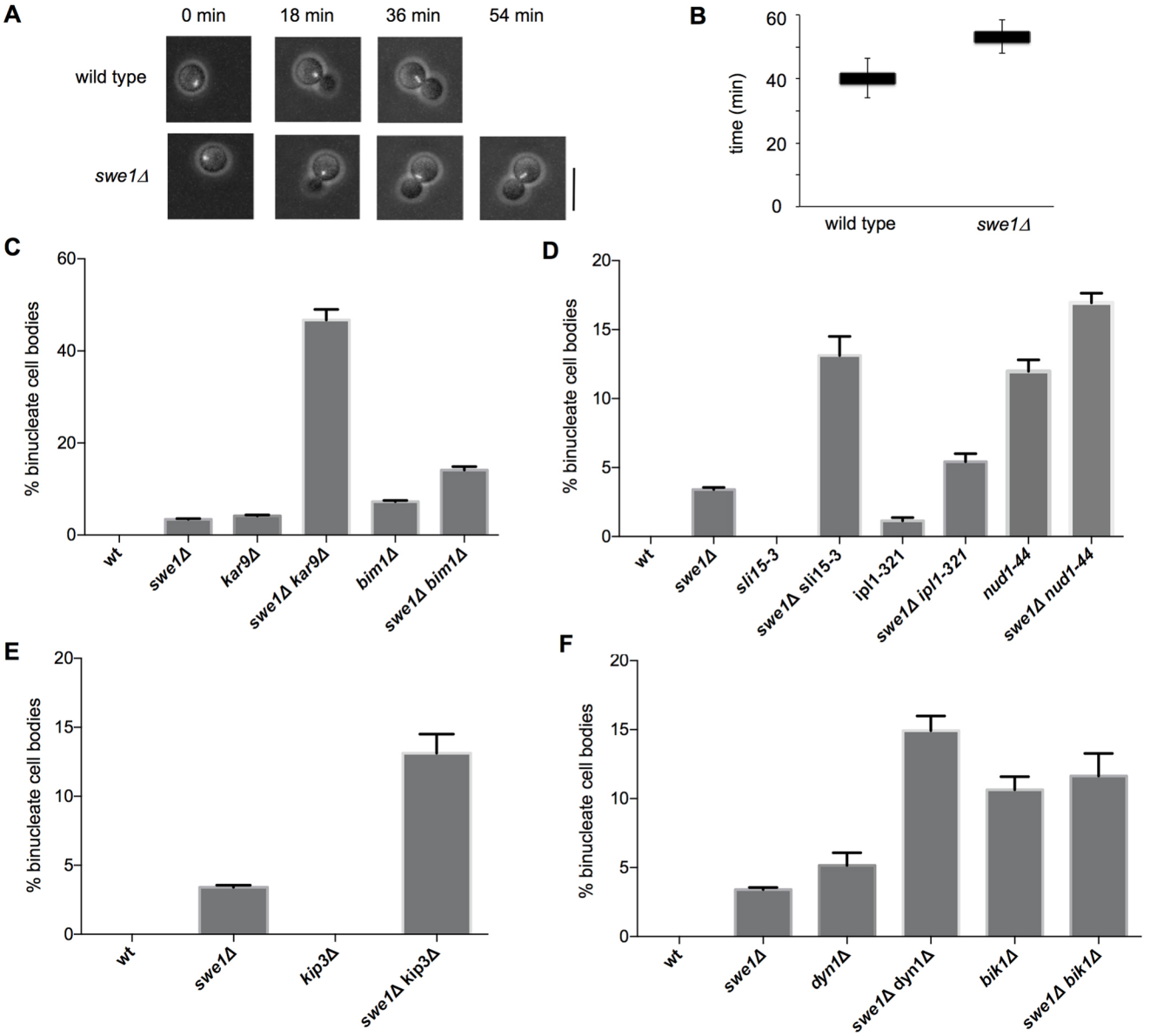

Fig. 1. The lack of Swe1 exacerbates spindle position defects. (A) Wild-type and *swe1Δ* cells expressing Tub1-GFP were arrested in G1 with α-factor and plated on glucose synthetic medium plates for time-lapse analysis (0 min). Images were taken every 3 min for 90 min. Scale bar: 5 µm. (B) The time required for correct spindle positioning at the bud neck was measured in 70 living cells for each strain captured as described in A. Unpaired *t*-test, P=0.0137. (C-F) Three independent cultures of strains with the indicated genotypes were grown at 25°C and shifted at 37°C for 3 h (C,D) or 14°C for 16 h (E,F). Samples were collected, fixed in ethanol and stained with DAPI. The percentage of binucleate cell bodies in total number of cells was scored (n>200). Statistical significance was analysed by two-way ANOVA Tukey's multiple comparisons test and the results are shown in Table S1. Data are mean±s.d.

(Bodenmiller and Aebersold, 2010), so we wondered if Bik1 was a phosphoprotein and if Swe1 was involved in its phosphorylation. We prepared native protein extracts from wild-type cycling cells and analysed the electrophoretic mobility of Bik1 by SDS-PAGE and western blotting with anti-Bik1 antibodies. We observed that Bik1 migrates as multiple bands specifically recognized by the anti-Bik1 antibodies (Fig. 2A, input lane). To understand if the slowly migrating Bik1 species might be due to phosphorylation events, we immunoprecipitated Bik1 from native protein extracts of wild-type cycling cells and treated them with lambda phosphatase. As shown in Fig. 2A, the slowly migrating species disappeared after the phosphatase treatment (PP lane), indicating that they represent phosphorylated Bik1. To better understand if this phosphorylation is regulated during the cell cycle, wild-type cells were inoculated in YEPD, arrested in G1 with α-factor and released in fresh medium. At 90 min after release, when more than 90% of cells were budded, we re-added α-factor to the culture to arrest cells in the next G1 phase in order to analyse a single cell cycle. Samples were taken at different time points after release to monitor the kinetics of DNA replication, budding, mitotic spindle formation, nuclear division and Bik1 phosphorylation. The wild-type strain progressed normally through the cell cycle according to FACS analysis of DNA content and other cell cycle kinetics (Fig. 2B); interestingly, in G1 and in early S phase Bik1 appears in its unphosphorylated form, then, ∼60 min after release, when the bipolar spindle is formed, the phosphorylated form appears. Later, as the cells elongate the spindle and divide, Bik1 gets dephosphorylated (Fig. 2C). These data indicate that Bik1 is phosphorylated in a cell-cycle-dependent

Journal of Cell Science (2018) 131, jcs213520. doi:10.1242/jcs.213520

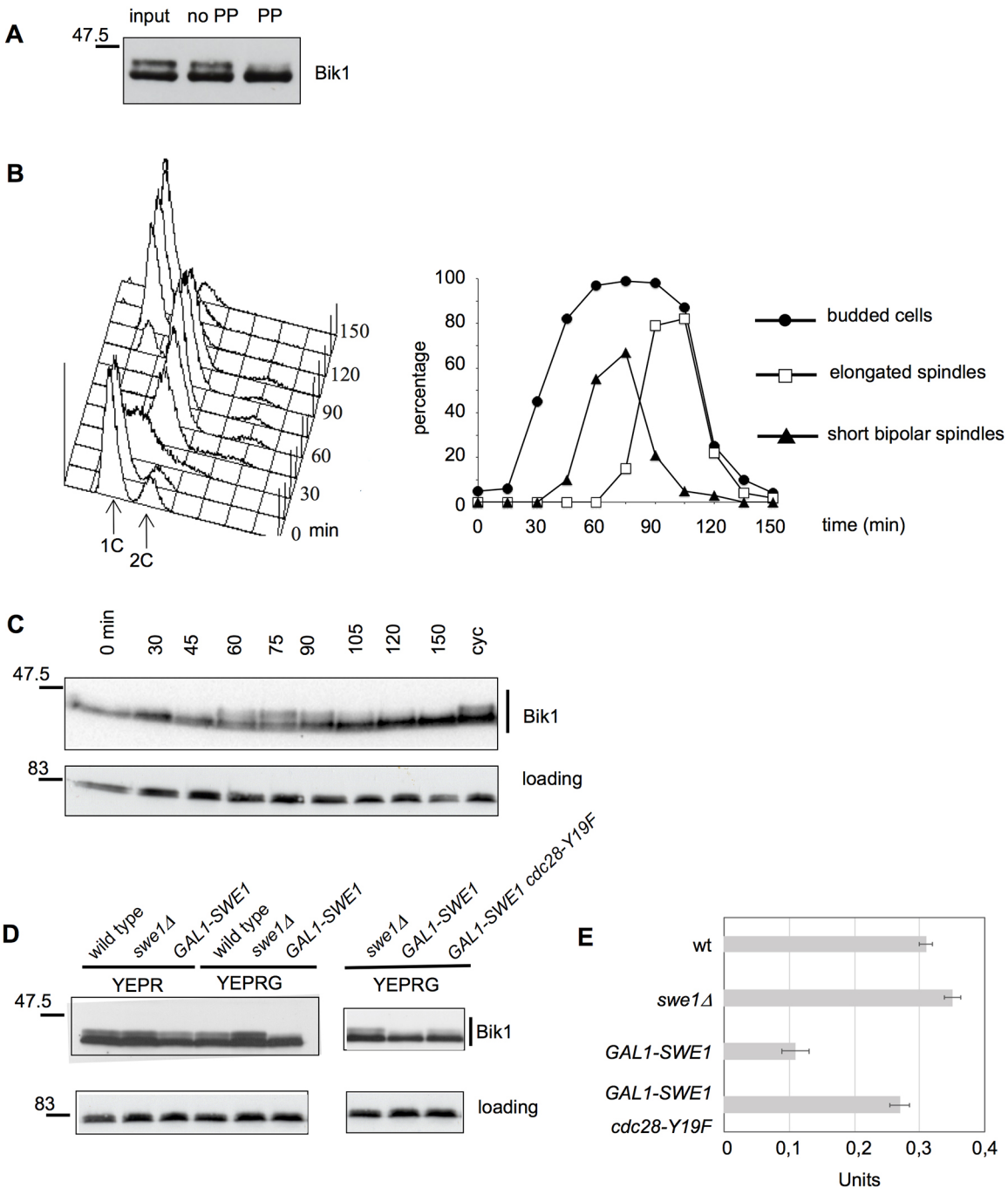

Fig. 2. Bik1 is a phosphoprotein. (A) Native protein extracts of wild-type cells (input) were immunoprecipitated with anti-Bik1 antibodies and the immunoprecipitate was incubated for 30 min at 30°C with 20 units/µl λ phosphatase (PP) or with reaction buffer (no PP). Samples were analysed by western blot analysis using anti-Bik1 antibodies. (B,C) Exponentially growing culture of wild-type cells was arrested in G1 by α-factor and released in fresh medium (0 min). At the indicated times after release, cell samples were collected for analysis of DNA content, budding and mitotic spindle formation and elongation (B) and to analyse Bik1 phosphorylation by western blot analysis (C) using anti-Bik1 antibodies. Swi6 is the loading control. (D) Wild-type, *swe1Δ* and *GAL1-SWE1* or *swe1Δ*, *GAL1-SWE1* and *GAL1-SWE1cdc28-Y19F* cells were inoculated in YEPR and shifted to YEPRG for 3 h. Then, samples were collected both from YEPR and YEPRG cultures to analyse Bik1 phosphorylation by western blot analysis using anti-Bik1 antibodies. Swi6 is the loading control. (E) Densitometric analysis of phosphorylated Bik1 over total Bik1 (pBik1/tot), the graph shows the results of four independent blots. Data are mean±s.d.

manner and that its dephosphorylation is concomitant with spindle elongation.

In order to test if Swe1 is involved in Bik1 phosphorylation, wild-type, *swe1Δ* and *GAL1-SWE1* cells were inoculated in YEPR and shifted in galactose-containing medium (YEPRG) for 3 h to induce Swe1 overproduction. Samples were collected from both YEPR and YEPRG cultures to assess Bik1 phosphorylation by western blot analysis. In wild-type cells, Bik1 appears as multiple bands as a result of phosphorylation events (see also Fig. 2A). Surprisingly, Bik1 phosphorylation did not increase in cells with high Swe1 levels with respect to the wild type, rather it decreased; in addition, it was raised in *swe1Δ* cells compared with wild-type levels (Fig. 2D,

Journal of Cell Science (2018) 131, jcs213520. doi:10.1242/jcs.213520

left panel, E). These results indicate that Swe1 does not directly phosphorylate Bik1, as suggested by previously published results (Bodenmiller and Aebersold, 2010).

As Bik1 contains a CDK consensus sequence, and since Swe1 is involved in CDK activation, we asked if the lack of Bik1 phosphorylation in Swe1-overproducing cells could be due to the inhibitory effect of Swe1 on Cdc28. To answer this question, we analysed Bik1 phosphorylation in cells with high Swe1 levels and expressing a non-phosphorylatable allele of Cdc28, *cdc28-Y19F*, as the only source of Cdc28 (McMillan et al., 1999). We included *swe1Δ* cells as a positive control because, as this allele produces a Cdc28 variant that should not be inhibited by Swe1, it mimics the absence of Swe1 as far as Cdc28 phosphorylation is concerned. For this purpose, exponentially growing cultures of *GAL1-SWE1*, *GAL1-SWE1 cdc28-Y19F* and *swe1Δ* cells were grown in YEPR and shifted in galactose-containing medium for 3 h, then samples were collected to analyse Bik1 phosphorylation as described above. The Y19F substitution was not able to restore Bik1 phosphorylation in *SWE1*-overexpressing cells as it does in *swe1Δ* cells; however, in *GAL1-SWE1 cdc28-Y19F* cells, Bik1 is more phosphorylated than it is in *SWE1*-overproducing cells (Fig. 2D, right panel, E). This indicates that Cdc28 could contribute to Bik1 phosphorylation together with other protein kinase(s) and that Swe1 partially influences Bik1 phosphorylation through CDK regulation. However, since Bik1 phosphorylation changes during the cell cycle (Fig. 2B) and both *SWE1* overexpression and Cdc28Y19F have an impact on cell cycle progression, we have to consider that this could influence our results.

Mih1 is involved in spindle elongation

We previously reported that cdc28-Y19F variant does not restore proper spindle elongation in *SWE1*-overexpressing cells (Raspelli et al., 2015), supporting the idea that Swe1 plays a role in this process by acting on other target/s. Since Bik1 does not seem to be directly phosphorylated by Swe1, we used an alternative strategy to search for Swe1 targets involved in spindle dynamics. We took advantage of *SWE1*-overexpressing cells (*GAL1-SWE1*), whose viability is compromised in galactose-containing medium – a condition in which they arrest with an elongated bud and monopolar spindle (Raspelli et al., 2015). The toxic effect of *GAL1-SWE1* is probably due to uncontrolled kinase activity of Swe1, since overexpression of a Swe1 kinase-dead version (GAL1-Swe1K-473A, *GAL1-swe1-kd*) does not cause cell lethality (Fig. 3A). With the aim of finding Swe1 targets, we analysed several conditions that could restore mitotic spindle elongation and therefore viability of *SWE1*-overexpressing cells. Interestingly, we found that the overproduction of the polo-like kinase Cdc5, which plays several roles during the cell cycle and promotes mitosis (van de Weerdt and Medema, 2006), partially restores the viability of *GAL1-SWE1* cells on galactose-containing plates (Fig. 3A).

It has been described that Cdc5 promotes SPB separation by promoting Cdh1 degradation (Simpson-Lavy et al., 2015) so we tested if *GAL1-CDC5* could rescue *GAL1-SWE1* lethality by this process. Conversely, *cdh1* deletion allows SPB separation in *GAL1-SWE1* cells, but not their viability in galactose-containing plates (Fig. S1).

Among other protein kinases, Cdc5 has a positive role in Swe1 degradation (Asano et al., 2005); we therefore asked if the partial ability of *GAL1-SWE1 GAL1-CDC5* cells to form colonies on YEPRG plates could be due to lower levels of Swe1 in these cells with respect to *GAL1-SWE1* cells. For this purpose, we constructed a strain in which the coding sequence of *SWE1* under the *GAL1* promoter was fused in-frame with 3PK epitopes recognized by commercial antibodies, which allowed us to analyse Swe1 levels by western blot analysis. *GAL1-SWE1-3PK* and *GAL1-SWE1-3PK GAL1-CDC5* cells were inoculated in YEPR, arrested in G1 with α-factor and released in YEPRG. Samples were taken at different time points after release to monitor the kinetics of DNA replication by FACS analysis and Swe1 levels by western blot analysis (Fig. 3B,C). Importantly, Swe1 levels remained high until the end of the experiment in both *GAL1-SWE1* and *GAL1-SWE1 GAL1-CDC5* cells (Fig. 3C), indicating that the restored viability of cells overexpressing both *CDC5* and *SWE1* (Fig. 3A) is not due to a decrease in Swe1 levels. Interestingly, the patterns of Swe1 phosphorylation are different between the two strains. In particular, in *CDC5*-overexpressing cells, Swe1 is more phosphorylated, consistent with the fact that Cdc5 phosphorylates Swe1 (Asano et al., 2005). Since Swe1 phosphorylation is required for its inactivation, and its kinase activity is required for the toxic effect of *GAL1-SWE1* (Fig. 3A), we cannot rule out the possibility that high Cdc5 levels partially inactivate Swe1 and that this is sufficient to restore the viability of Swe1-overproducing cells.

Mih1 is the protein phosphatase that counteracts the action of Swe1 on Cdc28; it reverses the inhibitory phosphorylation on Y19 of Cdc28 (Russell et al., 1989), leading to Cdk1 activation and entry into mitosis. Interestingly, we observed that deletion of *MIH1* completely abolished the viability of *GAL1-SWE1 GAL1-CDC5* cells (Fig. 4A), indicating that the presence of Mih1 is essential for these cells to survive. To better understand in which cellular compartment Mih1 performs its essential function, we took advantage of two mutated versions of Mih1: one that localizes exclusively in the cytoplasm (Mih1-NLS^{-}) and the other in the nucleus (Mih1-NLS^{-SV40}) (Keaton et al., 2008). These two mutant proteins are expressed at similar levels (Keaton et al., 2008) and do not impair cell viability per se (Fig. S2). We observed that the presence of Mih1-NLS^{-}allows a partial suppression of *GAL1-SWE1 GAL1-CDC5 mih1Δ* lethality, whereas Mih1-NLS^{-SV40} does not (Fig. 4A). These data indicate that cytoplasmic targets of Mih1 might be required to allow Cdc5-dependent mitotic spindle elongation.

We therefore decided to investigate this aspect to better understand why *CDC5* overexpression allows *GAL1-SWE1* cells to form colonies on galactose-containing plates and the role of the protein phosphatase Mih1 in this process. Since Mih1 counteracts Swe1 phosphorylation on Cdc28 in order to allow Cdk1 activation, one can hypothesize that Mih1 supports *GAL1-SWE1 GAL1-CDC5* viability simply through Cdc28 dephosphorylation. If this is the case, the introduction of the *cdc28-Y19F* allele at the *CDC28* locus should be sufficient to allow spindle elongation in *GAL1-SWE1 GAL1-CDC5 mih1Δ* cells. To test this hypothesis, wild-type, *GAL1-SWE1*, *GAL1-SWE1 GAL1-CDC5*, *GAL1-swe1-kd, GAL1-SWE1 GAL1-CDC5 mih1Δ* and *GAL1-SWE1 GAL1-CDC5 mih1Δ cdc28-Y19F* cells were arrested in G1 with α-factor and released in galactose-containing medium. Samples were taken at different time points after release to monitor the kinetics of DNA replication by FACS analysis (Fig. S3A) and spindle assembly and elongation by immunofluorescence (Fig. 4B). As already described in literature, wild-type cells properly replicated their DNA and divided, while *SWE1*-overexpressing cells accumulated with 2C DNA content and monopolar spindles (Fig. S3, Fig. 4B; Raspelli et al., 2015). As for cell viability (Fig. 3A), the kinase activity of Swe1 is essential to cause spindle defects in the *GAL1-SWE1* strain, since *GAL1-swe1-kd* cells assembled and elongated the mitotic spindle similarly to wild-type cells (Fig. 4B and Fig. S3B). *GAL1-SWE1 GAL1-CDC5*

Journal of Cell Science (2018) 131, jcs213520. doi:10.1242/jcs.213520

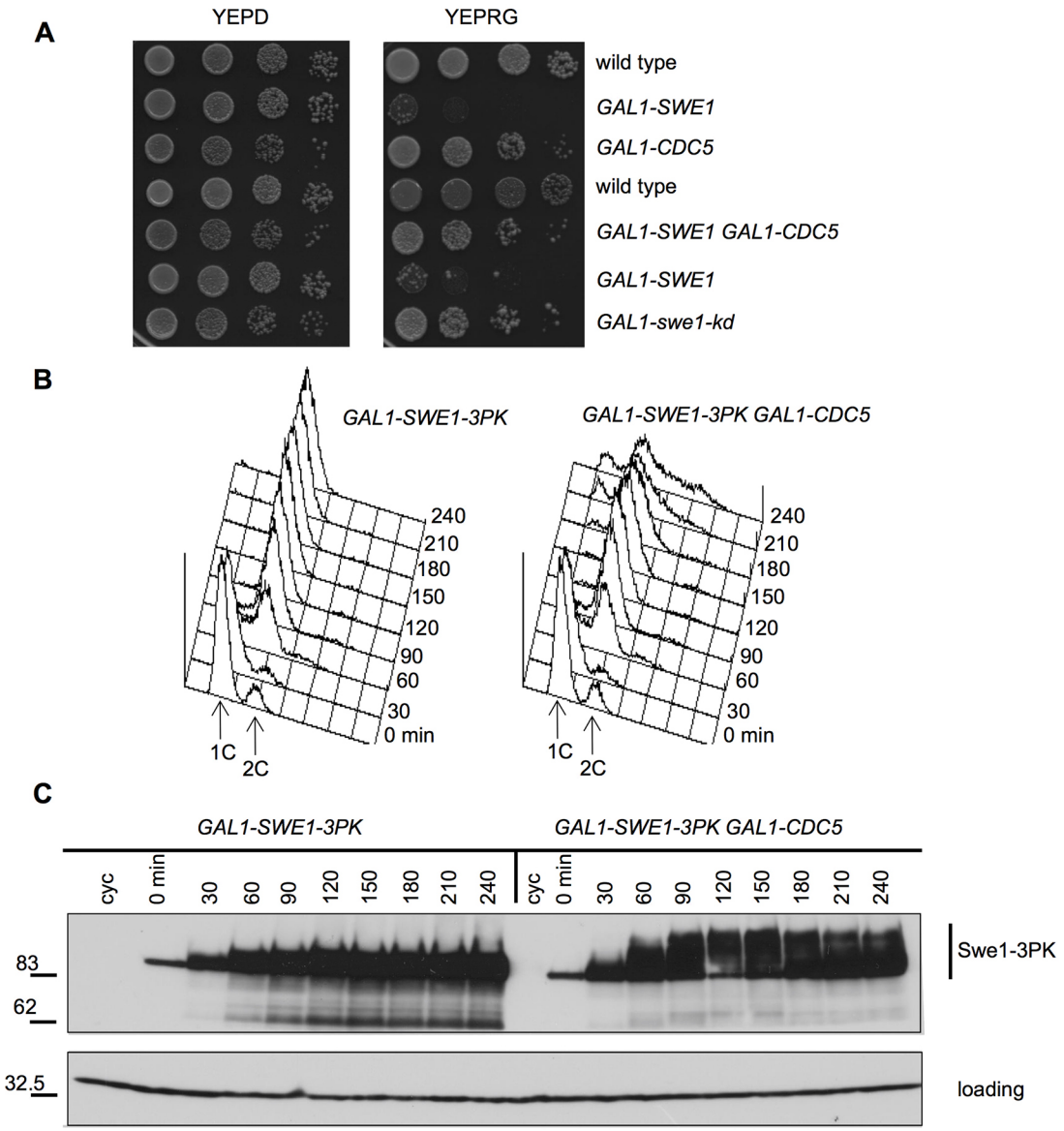

Fig. 3. *CDC5* overexpression partially restores viability of *SWE1*-overexpressing cells. (A) Serial dilutions of stationary phase cultures of strains with the indicated genotypes were spotted on YEPD or YEPRG plates which were then incubated for 2 days at 25°C. (B,C) Exponentially growing cultures of *GAL1-SWE1-3PK* and *GAL1-SWE1-3PK GAL1-CDC5* cells were arrested in G1 by α-factor in YPR and released from G1 arrest in YEPRG (2% galactose) at 25°C (0 min) to induce *SWE1* and *CDC5* overexpression. At the indicated times after release, cell samples were taken for FACS analysis of DNA content (B) and to determine Swe1 levels by western blot analysis with anti-PK antibodies (C). Pgk1 is the loading control.

cells partially elongated the mitotic spindle and divided (Fig. 4B,C), although less efficiently than wild-type cells did, as *CDC5* overexpression is partially toxic for cells (Fig. 3A; McMillan et al., 1999). Interestingly, cells overexpressing both *SWE1* and *CDC5* but lacking *MIH1* accumulated as budded cells with 2C DNA content, separated SPBs and with a short bipolar spindle that failed to elongate (Fig. 4B and Fig. S3). Therefore, the overexpression of *CDC5* is sufficient to allow SPB separation in *SWE1*-overexpressing cells, as expected since it promotes Cdh1 degradation (Simpson-Lavy et al., 2015) but the protein phosphatase Mih1 is required for these cells to elongate the mitotic spindle. Interestingly, the non-phosphorylatable *cdc28-Y19F* allele allows only a fraction of *GAL1-SWE1 GAL1-CDC5 mih1Δ* cells to elongate the spindle (Fig. 4B and Fig. S3B), indicating that the dephosphorylation of Cdc28 is not sufficient to restore proper spindle elongation in *GAL1-SWE1 GAL1-CDC5* cells in the absence of Mih1. Collectively, these results indicate that Mih1 has a positive role in spindle elongation, it might act on another unidentified cytoplasmic target(s) apart from Cdc28 and it works downstream of Swe1 and Cdc5.

To gain insight into the role of Mih1 on mitotic spindle elongation we performed time-lapse analysis of spindle dynamics in wild-type and *mih1Δ* cells expressing the Tub1-GFP variant. We did not observe significant differences between the kinetics of bipolar spindle assembly in the two strains, but the lack of Mih1 caused a delay in the process of elongation (10.54±1.88 min versus 16.50±3.55 min) (Fig. 4C,D and Movies 1 and 2). The difference between the two strains is significant (*P*-value obtained by unpaired test, $P<0.0001$) and further supports the hypothesis that Mih1 is important for mitotic spindle elongation even during normal cell

Journal of Cell Science (2018) 131, jcs213520. doi:10.1242/jcs.213520

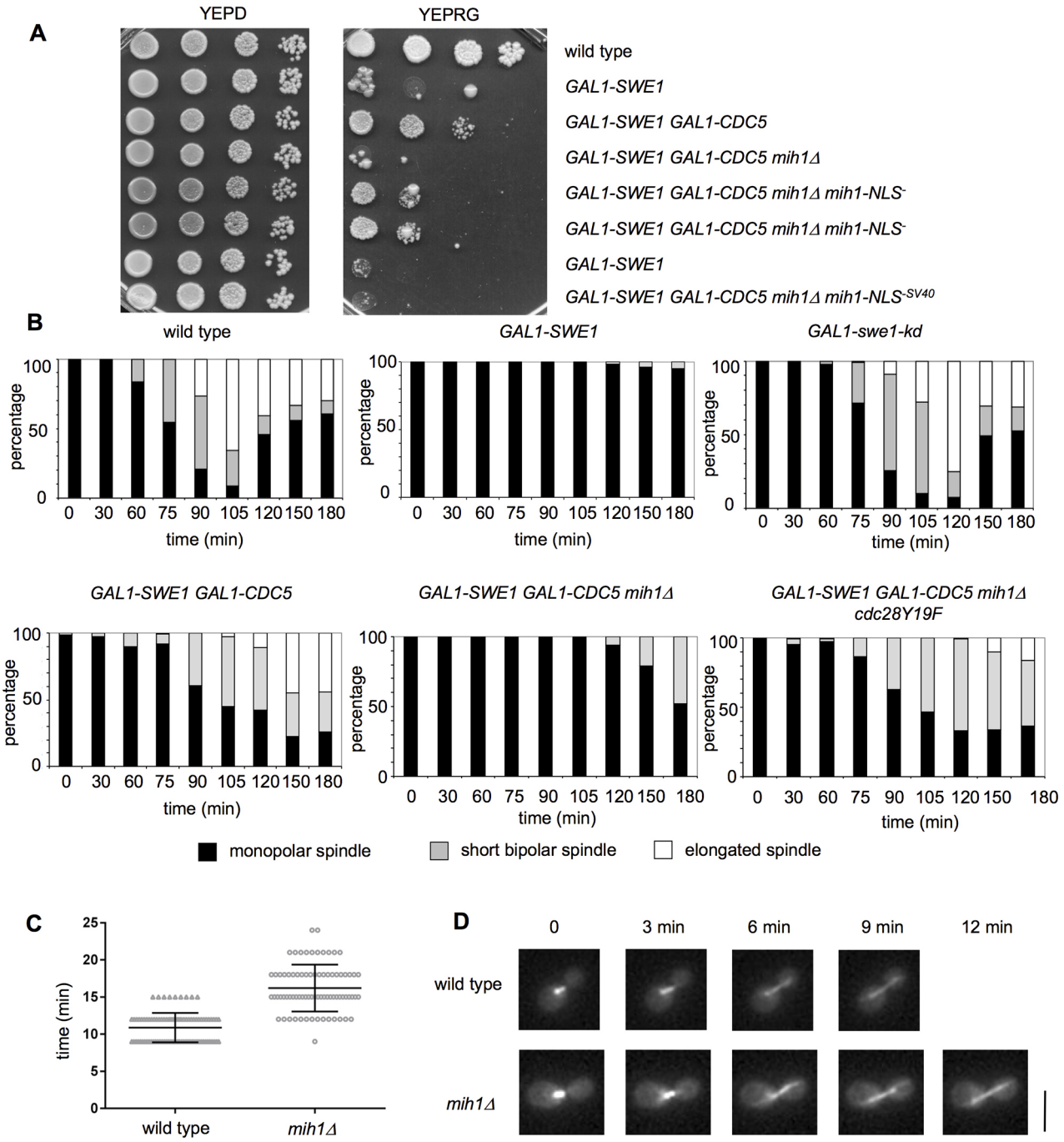

Fig. 4. Mih1 is required for mitotic spindle elongation. (A) Serial dilutions of stationary phase cultures of strains with the indicated genotypes spotted on YEPD or YEPRG plates and incubated for 2 days at 25°C. (B) Exponentially growing cultures of wild-type, *GAL1-SWE1*, *GAL1-SWE1 GAL1-CDC5*, *GAL1-swe1-kd*, *GAL1-SWE1 GAL1-CDC5 mih1Δ* and *GAL1-SWE1 GAL1-CDC5 mih1Δ cdc28Y19F* cells were arrested in G1 by α-factor in YEPR and released from G1 arrest in YEPRG (2% galactose) at 25°C (0 min) to induce *SWE1* and *CDC5* overexpression. At the indicated times after release, cell samples were taken to score mitotic spindle formation and elongation by immunofluorescence using anti-tubulin antibodies. Statistical significance was analysed by ordinary one-way ANOVA Dunnett's multiple comparisons test and the results are shown in Table S2. (C) Exponentially growing cultures of wild-type and *mih1Δ* cells, all expressing Tub1-GFP, were arrested in G1 by α-factor and plated on glucose synthetic medium for time-lapse analysis. Images were taken every 3 min for 3 h and time-lapse images were assembled to show mitotic spindle dynamics (Movies 1 and 2). The graph indicates the rate of mitotic spindle elongation scored in 150 cells for each strain. Statistical significance was analysed by unpaired *t*-test, $P<0.0001$. Data are mean±s.d. (D) Representative images taken from Movies 1 and 2 showing mitotic spindle dynamics in wild-type and *mih1Δ* cells. Scale bar: 5 µm.

growth. Moreover, we noticed that in a consistent fraction of *mih1Δ* cells (25% of *mih1Δ* vs 7% of wild-type cells, $n=100$) (Fig. S4), the short mitotic spindle moves between the mother and the bud before finally elongating, indicating that Mih1, like Swe1 (Fig. 1), could have a role in spindle positioning. Collectively, these results indicate that Mih1 has a positive role in spindle elongation, it might act on other unidentified cytoplasmic target(s) apart from Cdc28, and it acts downstream of Swe1 and Cdc5.

Journal of Cell Science (2018) 131, jcs213520. doi:10.1242/jcs.213520

Mih1 makes a complex with Bik1 and regulates its phosphorylation

We demonstrated that Mih1 is likely to have a positive role in promoting mitotic spindle elongation (Fig. 4) and since Bik1 dephosphorylation correlates with spindle elongation (Fig. 2B,C), we asked if Mih1 could promote this effect. To answer this question, exponentially growing wild-type and *mih1Δ* cells were arrested in G1 with α-factor and released in fresh medium. Samples were collected at different time points after release to monitor cell cycle progression by microscopy (Fig. S5B) and to analyse Bik1 phosphorylation by western blot analysis. In wild-type cells, the phosphorylated Bik1 band appears 60 min after release, similarly to the experiment shown in Fig. 2C; interestingly, the lack of Mih1 allows accumulation of phosphorylated Bik1 forms earlier and to a greater extent with respect to that in wild-type cells (Fig. 5A and Fig. S5A). In addition, we observed that the presence of a cdc28Y19F variant as the only source of Cdc28 does not restore proper Bik1 phosphorylation kinetics (Fig. 5B), indicating that Mih1 could be involved in Bik1 dephosphorylation. Consistent with the time-lapse experiment (Fig. 4C), we observed that *mih1Δ* cells show a delay in mitotic spindle elongation and that presence of the cdc28Y19F variant does not re-establish the correct kinetics.

We then performed a coimmunoprecipitation experiment to test if Bik1 and Mih1 form a complex *in vivo*. We prepared native protein extracts from cycling cells of wild-type strains expressing untagged or 3-HA-tagged Mih1 and we incubated them with Protein-A Sepharose bound to anti-HA antibodies. From western blot analysis of the bead-bound fraction, we observed that Mih1 could immunoprecipitate Bik1 specifically (Fig. 5D), indicating that they form a complex *in vivo* and suggesting that Mih1 might dephosphorylate Bik1.

Swe1 and Cdc5 control the balance between phosphorylated and unphosphorylated forms of Mih1

The experiments shown in Fig. 4 suggest that Mih1 is essential when levels of Swe1 and Cdc5 are high; this role is independent of its role in Cdc28 dephosphorylation and it acts downstream of Cdc5. In mammalian cells, the homologue of Cdc5, PLK, phosphorylates

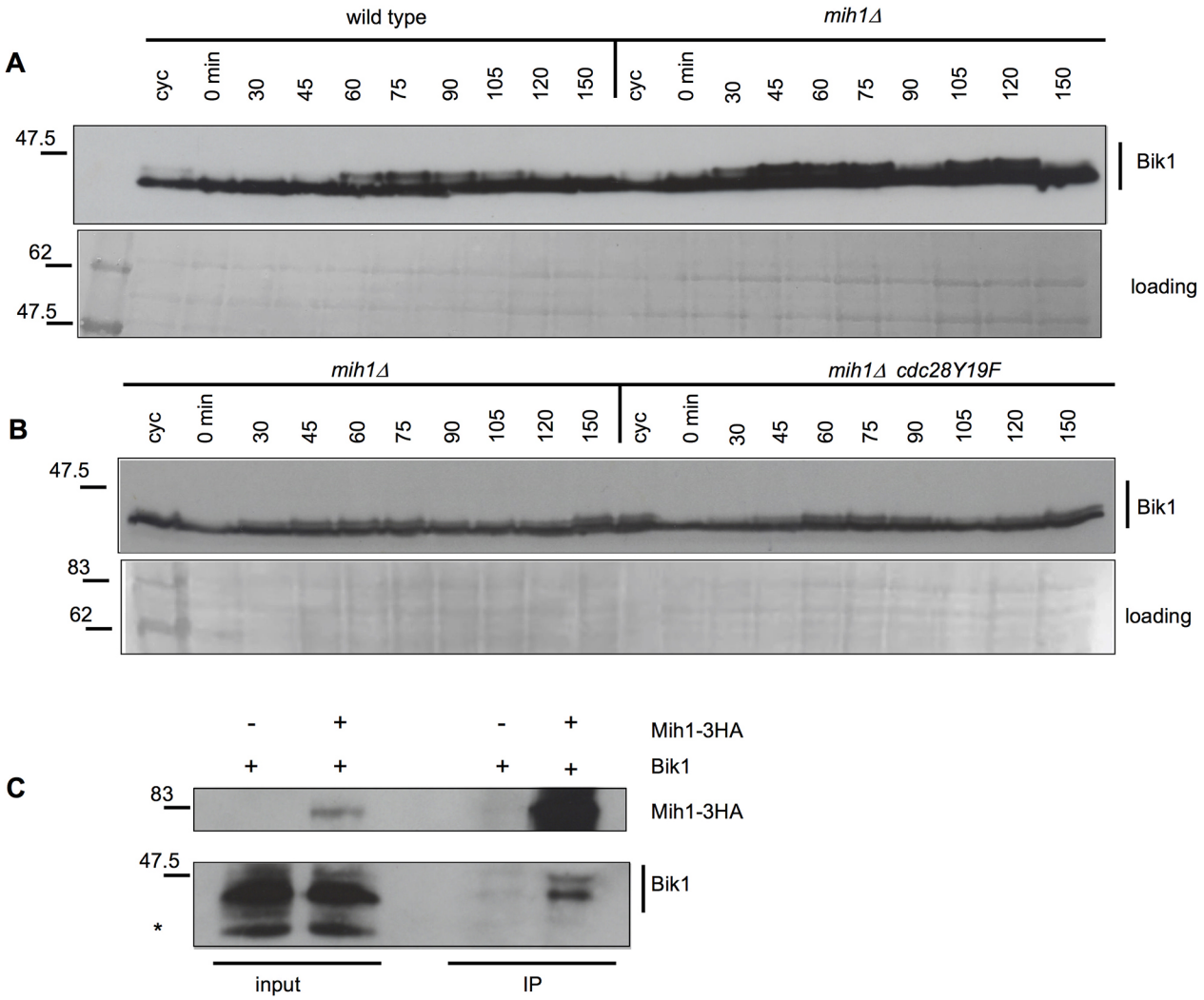

Fig. 5. Mih1 forms a complex with Bik1 and is involved in Bik1 dephosphorylation. (A,B) Exponentially growing cultures of wild-type, *mih1Δ* and *mih1Δ cdc28Y19F* were arrested in G1 by α-factor in YEPD and released from G1 arrest in fresh medium (0 min). At the indicated times after release, cell samples were taken to analyse Bik1 phosphorylation by western blot analysis using anti-Bik1 antibodies. Ponceau S staining of the filter before western blot processing shows total protein amount in each lane. (C) Protein-A beads bound to anti-HA antibodies were incubated with native protein extracts prepared from either exponentially growing wild-type or *MIH1-HA3* cells. Washed and boiled beads were subjected to SDS-PAGE followed by immunoblotting with Bik1 and anti-HA antibodies. The asterisk indicates a nonspecific band.

Journal of Cell Science (2018) 131, jcs213520. doi:10.1242/jcs.213520

CDC25B, which is the homologue of Mih1, thus promoting CDK activation and entry into mitosis (Lobjois et al., 2009, 2011) and one intriguing possibility is that Cdc5 could also regulate Mih1 in budding yeast. Therefore, we analysed Mih1 phosphorylation, taking advantage of *CDC5*-overexpressing cells and *cdc5-2* cells carrying a Cdc5-lack of function mutant and expressing a functional Mih1-3HA version.

MIH1-3HA and *MIH1-3HA GAL1-CDC5* cells were inoculated in YEPR, arrested in G1 with α-factor and released in YEPRG. At 90 min after release, when more than 90% of cells were budded, we re-supplied α-factor to the cultures to arrest cells in the next G1 phase, thus analysing a single cell cycle. Samples were taken at different time points after release to monitor the kinetics of DNA replication by FACS analysis and Mih1 levels and phosphorylation by western blot analysis. Wild-type cells expressing *MIH1-3HA* progressed normally through the cell cycle and arrested in the next G1 (Fig. 6A, left), while *CDC5*-overexpressing cells replicated their DNA but partially failed to divide (Fig. 6A, right), because high Cdc5 levels inhibit cytokinesis (Song and Lee, 2001). As Mih1 has several phosphorylation sites (Pal et al., 2008), it appears as a series of bands with different molecular weights. As shown in Fig. 6B, soon after release from G1 arrest, Mih1 is fully phosphorylated, whereas 45 min after release, the less-phosphorylated forms appeared, along with the appearance of the hyper-phosphorylated form. It is interesting to note that in both wild-type and *GAL1-CDC5* cells, the pattern of phosphorylation is almost the same during the whole time of the experiment, indicating that overexpression of *CDC5* does not change the balance between different Mih1 phosphorylation forms. Accordingly, Mih1 phosphorylated forms do not decrease in *cdc5-2* cells grown at 25°C and shifted for 3 h at 37°C, a restrictive temperature for the ts allele (Fig. 6C). These data indicate that the budding yeast Polo kinase Cdc5 probably does not directly phosphorylate Mih1.

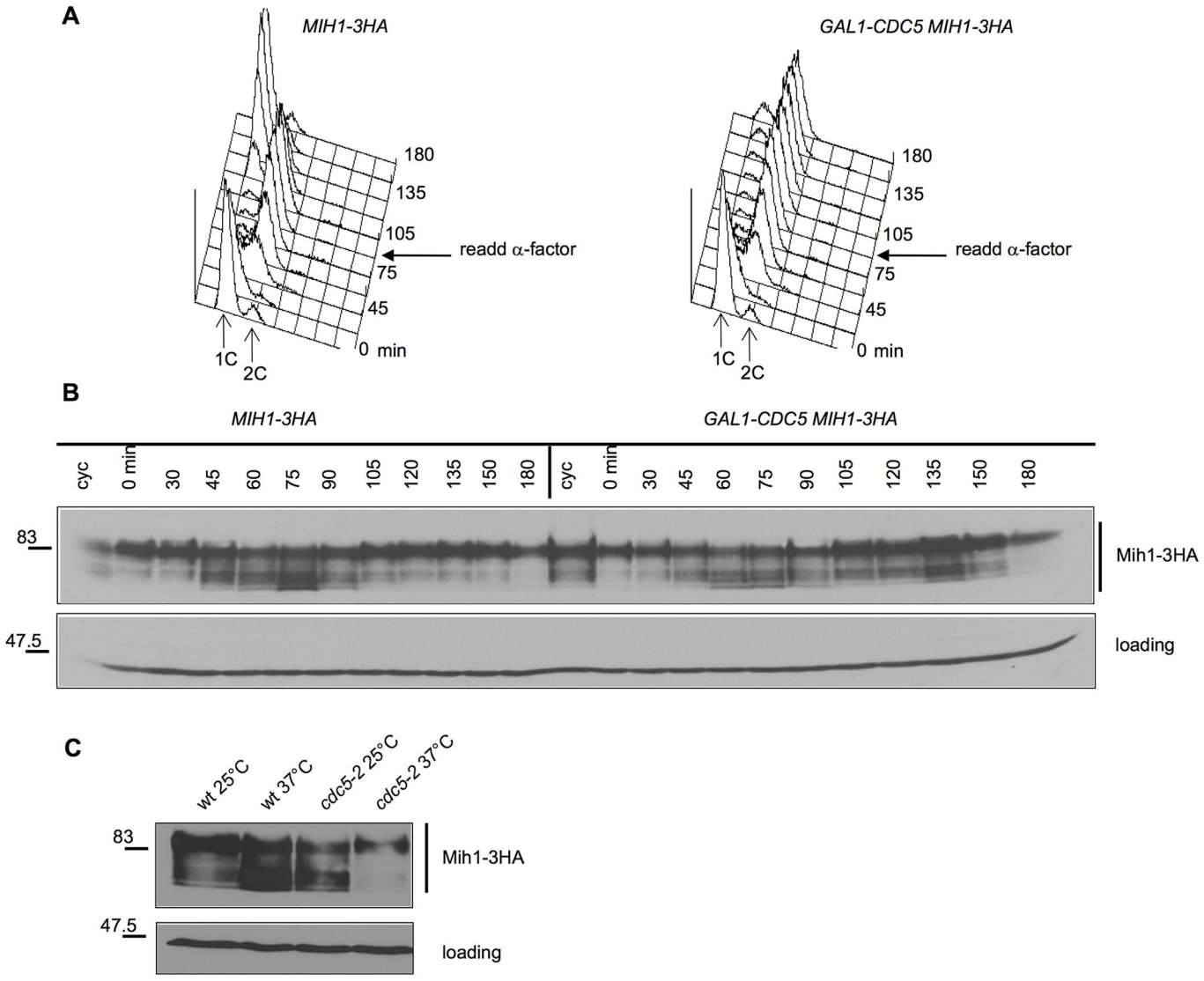

Fig. 6. Cdc5 does not directly phosphorylate Mih1. Exponentially growing cultures of *MIH1-3HA* and *GAL1-CDC5 MIH1-3HA* cells were arrested in G1 by α-factor in YEPR and released from G1 arrest in YEPRG (2% galactose) at 25°C (0 min) to induce *CDC5* overexpression. At the indicated times after release, cell samples were taken for FACS analysis of DNA content (A) and to determine Mih1 levels and modifications by western blot analysis with anti-HA antibodies (B). Pgk1 is the loading control. (C) Exponentially growing cultures of *MIH1-3HA* and *cdc5-2 MIH1-3HA* cells at 25°C were shifted to 37°C for 3 h and cell samples were taken to determine Mih1 levels by western blot analysis with anti-HA antibodies. Cdc11 is the loading control.

Journal of Cell Science (2018) 131, jcs213520. doi:10.1242/jcs.213520

We then asked if *SWE1* overexpression or the concomitant *SWE1* and *CDC5* overexpression changed the pattern of Mih1 phosphorylation, the latter being the condition in which Mih1 becomes essential for mitotic spindle elongation (Fig. 4C). *GAL1-SWE1 MIH1-3HA* and *GAL1-SWE1 GAL1-CDC5 MIH1-3HA* cells were inoculated in YEPR, arrested in G1 with α-factor and released in YEPRG. Samples were taken at different time points after release to monitor the kinetics of DNA replication and Mih1 levels and phosphorylation. Both strains behave as in the experiments previously described with respect to the kinetics of DNA replication (Fig. S6, compare with Fig. 3B); in *SWE1*-overexpressing cells, hyper-phosphorylated Mih1 persisted throughout the experiment but, interestingly, as a consequence of Cdc5 overproduction Mih1 hyper-phosphorylated forms disappeared (Fig. 7A). Since fully phosphorylated Mih1 is not functional (Pal et al., 2008), our data indicate that Swe1 overproduction might inhibit Mih1, while the concomitant presence of high levels of Cdc5 might restore the proper balance between phosphorylated and unphosphorylated forms of Mih1 and likely also its functionality.

To better understand if Swe1 could be directly involved in Mih1 regulation, we performed a co-immunoprecipitation experiment using protein extracts prepared from cycling cells of strains expressing Swe1-3PK and Mih1-3HA. Indeed, Swe1 could specifically immunoprecipitate Mih1 (Fig. 7B), indicating that they form a complex *in vivo* and suggesting that Swe1 might phosphorylate Mih1.

DISCUSSION

Mitotic spindle function is crucial for proper genetic material partitioning between mother and daughter cell, so its dynamics are finely regulated. It is well known that Swe1 is responsible for an inhibitory phosphorylation on the protein kinase Cdc28; however, some researchers suggest that Swe1 has other targets (Mahajan et al., 2012; Raspelli et al., 2015; Lengefeld et al., 2017). We previously showed that Swe1 has a role in the control of the mitotic spindle independently of its role on Cdc28 phosphorylation (Raspelli et al., 2015). In this paper, we investigated the role of Swe1 in mitotic spindle dynamics and we showed that it promotes spindle positioning, acting in parallel to Ipl1, Sli15, Nud1, Kar9, Bim1 and Dyn1 and in cooperation with the plus-end MAP Bik1. Here, we show that Bik1 is post-translationally modified by phosphorylation and that this modification is cell cycle dependent and correlates with bipolar spindle formation and elongation. Interestingly, a phosphoproteomic analysis on chip array identified Bik1 as a protein phosphorylated by Swe1 (Bodenmiller and Aebersold, 2010), but surprisingly, we found that Bik1 phosphorylation decreased in the presence of high Swe1 levels with respect to the wild-type protein, whereas it increased in *swe1Δ* cells, indicating that Swe1 controls Bik1 phosphorylation but does not directly phosphorylate it. Bik1 has a consensus site for CDK phosphorylation and, importantly, we showed that in Swe1-overexpressing cells, Bik1 phosphorylation was not completely restored by a Cdc28 variant that could not be inhibited by Swe1, indicating that other protein kinase(s) could be responsible for this residual phosphorylation. However, since it has been shown that cells expressing a non-phosphorylatable Cdc28 variant have an altered Cdc28 mitotic activity that results in defective APC activation and therefore a delay in mitotic exit (Rudner et al., 2000 and Rudner and Murray, 2000), we cannot exclude that this has an impact on Bik1 phosphorylation, since we showed that it correlates with spindle dynamics.

Interestingly, while searching for mutants that suppress the lethality of *SWE1*-overexpressing cells, we observed that high levels of the Polo-like kinase Cdc5 were sufficient to allow mitotic spindle elongation and to partially restore viability of *SWE1*-overexpressing cells. Importantly, this is not due to a reduction in Swe1 levels, but a partial inactivation of Swe1 through phosphorylation by Cdc5 could contribute to this process. In accordance with this hypothesis, the overexpression of a Swe1 kinase-dead version does not impair cell viability or mitotic spindle dynamics. In this context, we can hypothesize that Swe1 blocks some spindle elongation-promoting factor and that Cdc5 overexpression allows its activation though partial Swe1 inhibition. Surprisingly, lack of the protein phosphatase Mih1 completely abolished spindle elongation and cell division of *GAL1-SWE1 GAL1-CDC5* cells in galactose-containing medium and, consistently, their viability on YEPRG plates. Interestingly, *GAL1-SWE1 GAL1-CDC5 mih1Δ* cells arrested in galactose-containing medium with short bipolar spindles, and not with monopolar spindles as in *GAL1-SWE1* cells. Given that Cdc5 promotes SPB separation by Cdh1 degradation (Simpson-Lavy et al., 2015), it is not surprising that overexpression of *CDC5* is sufficient to allow SPB separation in *SWE1*-overexpressing cells but, importantly, the protein phosphatase Mih1 is required for these cells to elongate the mitotic spindle. This suggests that high levels of Cdc5 could suppress the spindle elongation defect of *SWE1*-overexpressing cells acting through the phosphatase Mih1 and that Mih1 essential function occurs after SPB separation. We observed that neither the expression of a non-phosphorylatable variant of Cdc28, as the only source of Cdc28 in the cells, nor the expression of a Mih1 variant that localizes exclusively in the nucleus was sufficient to restore either proper spindle elongation (Cdc28-Y19F) or viability (Mih1-NLS^{SV40}) of *GAL1-SWE1 GAL1-CDC5 mih1Δ* cells. These data can support the hypothesis that the dephosphorylation of an unidentified cytoplasmic Mih1 target(s) might be required for spindle elongation and cell viability in the presence of high levels of Swe1 and Cdc5.

We also characterized the role of Mih1 in mitotic spindle dynamics in physiological conditions and, according to previous works, we observed that the lack of Mih1 induces a delay in spindle elongation (Lianga et al., 2013) and problems in spindle positioning. These phenotypes correlate with the observation that the lack of Mih1 also leads to the accumulation of phosphorylated Bik1 in the presence of a non-phosphorylatable variant of Cdc28 and that Mih1 and Bik1 form a complex *in vivo*, indicating a direct role of Mih1 in mitotic spindle elongation possibly acting through the MAP Bik1. Expression of the *cdc28Y19F* allele does not cause major defects in cell cycle progression in normal conditions (Sorger and Murray, 1992; Raspelli et al., 2015); however, we must consider that it has a reduced mitotic Cdc28 activity that has an impact on APC phosphorylation and activation, spindle elongation and mitotic exit (Rudner et al., 2000 and Rudner and Murray, 2000), and it might therefore have unexpected effects in different genetic backgrounds or growth conditions. We favour the hypothesis that Swe1 and Mih1 also modulate spindle dynamics directly rather than only indirectly by modulating Cdk1 activity, but we cannot exclude the latter possibility.

As PLK, the homologue of Cdc5 in mammalian cells, phosphorylates CDC25B, the homologue of Mih1, in order to promote CDK activation and entry into mitosis (Lobjois et al., 2009, 2011), we reasoned that Cdc5 could also be responsible for Mih1 phosphorylation in budding yeast. However, our data indicate that, differently from mammalian cells, in budding yeast the Polo-like

Journal of Cell Science (2018) 131, jcs213520. doi:10.1242/jcs.213520

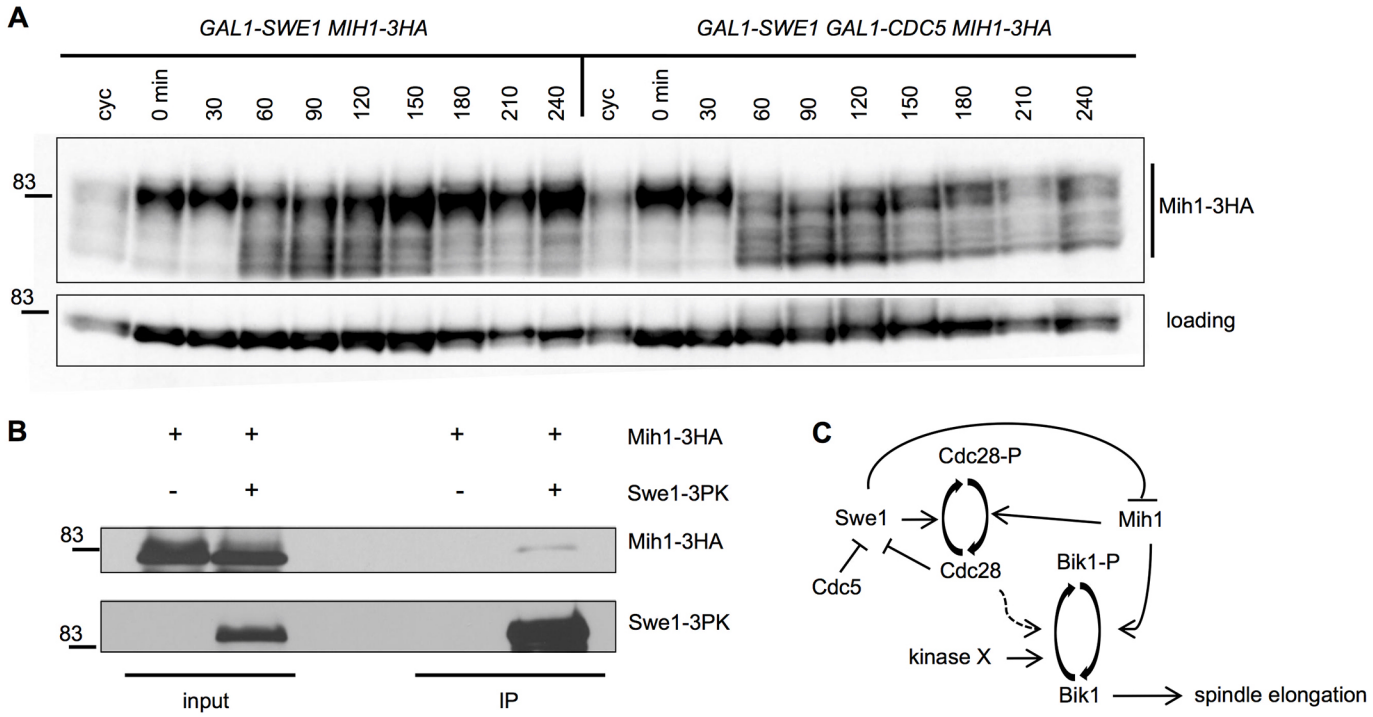

Fig. 7. Swe1 forms a complex with Mih1 and it is involved in its phosphorylation. (A) Exponentially growing cultures of *GAL1-SWE1 MIH1-3HA* and *GAL1-SWE1 GAL1-CDC5 MIH1-3HA* were arrested in G1 by α-factor in YEPR and released from G1 arrest in YEPRG (2% galactose) at 25°C (0 min) to induce *CDC5* and *SWE1* overexpression. At the indicated times after release, cell samples were taken to determine Mih1 levels by western blot analysis with anti-HA antibodies. Swi6 is the loading control. (B) Protein-A beads bound to anti-PK antibodies were incubated with native protein extracts prepared from either exponentially growing *MIH1-HA3* or *MIH1-HA3 SWE1-PK3* cells. Washed and boiled beads were subjected to SDS-PAGE followed by immunoblotting with anti-PK and anti-HA antibodies. (C) Cdc28 and Cdc5 both phosphorylate and inhibit Swe1, which, in turn, promotes inhibitory phosphorylation of Cdc28 and Mih1. Bik1 is likely to be phosphorylated by Cdc28 (dashed line) and by another unidentified protein kinase (kinase X) whereas Mih1 promotes Bik1 dephosphorylation and mitotic spindle elongation.

kinase is not likely to phosphorylate Mih1. In this context, our findings are consistent with a genetic and bioinformatics study in which a Cdc5 inhibition resulted in an upshift, rather than in a downshift, of Mih1 electrophoretic mobility (Snead et al., 2007). However, we found that *SWE1* overexpression causes the accumulation of fully phosphorylated Mih1 and that concomitant *CDC5* overexpression restores the proper balance between Mih1 phosphorylation forms. This is very important because a change in Mih1 phosphorylation changes its activity: in fact, both the fully phosphorylated and the not phosphorylated forms of Mih1 are inactive (Pal et al., 2008). Moreover our coimmunoprecipitation experiment shows that Swe1 and Mih1 form a complex *in vivo*, indicating that Swe1 could phosphorylate Mih1 and lead to inhibition of the phosphatase.

Our data fit into a model in which, in addition to its role in the Swe1-Cdc28-Mih1 pathway, Swe1 also controls Mih1, which, in turn, activates Bik1 and spindle elongation. Given that Mih1 has a positive role in promoting spindle elongation, we speculate that dephosphorylated Bik1 promotes this process, as depicted in Fig. 7C. To summarize, in this study we show that Swe1 and Mih1 are involved either directly or indirectly, through the control of Cdc28Y18 phosphorylation, in the regulation of mitotic spindle dynamics. In addition, we demonstrate that the protein kinases Swe1 and Cdc5 control the balance between phosphorylated and unphosphorylated forms of Mih1 and that Mih1 is important for mitotic spindle elongation in wild-type cells and essential in *SWE1*- and *CDC5*-overexpressing cells. In particular, our data indicate that Swe1 and Mih1 are both involved, directly or indirectly, in controlling the phosphorylation state of the microtubule binding protein Bik1, an important player in mitotic spindle orientation, stability and elongation. Since these proteins are all conserved from yeast to humans and since Bik1 is the homologue of CLIP-170, that plays a similar role in MT dynamics in human cells (Bieling et al., 2008), our findings are relevant to understand the complex functioning of the mitotic apparatus in multicellular eukaryotes.

MATERIALS AND METHODS

Strains, media and reagents, genetic manipulations

All yeast strains (Table S3) were derivatives of W303 (*ade2-1, trp1-1, leu2-3,112, his3-11,15, ura3, ssd1*). α-factor (Sigma-Aldrich) was used at 2 µg/ml or 10 µg/ml and, unless differently stated, cells were grown at 25°C in YEP (1% yeast extract, 2% bactopeptone, 50 mg/l adenine) medium supplemented with 2% glucose (YEPD) or 2% raffinose (YEPR) and 2% raffinose+1% galactose (YEPRG). Standard techniques were used for genetic manipulations (Sherman, 1991). Gene deletions were generated by one-step gene replacement (Maniatis et al., 1992). One-step tagging techniques were used to create 3PK-tagged Swe1 variant and Mih1-3HA (Wach et al., 1994). All gene replacements and tagging were controlled by PCR-based methods or Southern blot analysis.

Fluorescence microscopy

In situ immunofluorescence was performed on formaldehyde-fixed cells and carried out as previously described (Cassani et al., 2014). Nuclei were visualized by staining with 0.05 µg/ml DAPI. To detect spindle formation and elongation, α-tubulin immunostaining was performed with the YOL34 monoclonal antibody (1:100, Santa Cruz Biotechnology, cat. no. sc-53030)

followed by indirect immunofluorescence using Rhodamine-conjugated anti-rat Ab (1:500, Thermo Fisher, cat. no. 31680). Digital images were taken with a Leica DC350F charge-coupled device camera mounted on a Nikon Eclipse 600 and controlled by Leica FW4000 software or with the MetaMorph imaging system software on a fluorescent microscope (Eclipse 90i; Nikon), equipped with a charge-coupled device camera (Coolsnap, Photometrics) with an oil 100×0.5-1.3 PlanFluor objective (Nikon). Fluorescence analysis on living cells was performed as previously described (Fraschini, 2017). For time-lapse movies, cells were grown in synthetic complete medium+2% glucose and arrested in G1 by α- factor; cells were then collected, released and imaged on agar in synthetic complete medium+2% glucose using a Delta Vision Elite imaging system (Applied Precision) based on an IX71 inverted microscope (Olympus) with a camera CoolSNAP HQ2 from Photometrics, and a UPlanApo 60× (1.4 NA) oil immersion objective (Olympus). Every 3 min five *Z*-stacks at 1.2 µm intervals were taken for each fluorescent channel and projected onto a single image per channel using Fiji software (Schindelin et al., 2012). In Fig. 1A, time zero corresponds to the release from the block.

Protein extracts and analysis

For monitoring Bik1, Cdc11, Mih1, Pgk1, Swe1 and Swi6 levels total protein extracts were prepared by TCA precipitation as previously described (Raspelli et al., 2011). Co-immunoprecipitations were performed as previously described (Raspelli et al., 2015), except that cells were lysed in 50 mM Tris-HCl, pH 7.5, 150 mM NaCl, 10% glycerol, 1% NP40, 1 mM sodium orthovanadate and 60 mM β-glycerophosphate, supplemented with a cocktail of protease inhibitors (Complete mini, Roche). The phosphatase treatment (Fig. 2A) was performed as described (Raspelli et al., 2011), except that Bik1 was immunoprecipitated from 1 mg of clarified extracts upon incubation with anti-Bik1 antibodies (gift from Prof. Tim Huffaker, Cornell University Ithaca, NY) for 1 h at 4°C. For western blot analysis, proteins were transferred to Protran membranes (Schleicher and Schuell) and probed with monoclonal anti-HA (1:3000, Santa Cruz, cat. no. sc-57592), anti-PK (1:3000, Bio-Rad, cat. no. MCA1360), anti-Pgk1 (1:40,000, Molecular Probes, cat no. 459250), anti-Cdc11 (1:3000, Santa Cruz, cat no. sc-7170) anti-Swi6 (1:100,000), gift from Prof. Simonetta Piatti (CNRS, Montpellier, France) and anti-Bik1 antibodies (1:5000), gift from Prof. Tim Huffaker (Cornell University Ithaca, NY). Secondary antibodies were purchased from Amersham and proteins were detected using an enhanced chemiluminescence system according to the manufacturer (Amersham, cat. no. RPN2232).

Statistical analyses and other techniques

For experiments shown in Figs 1C-F, 2 and 4, at least 200 cells were counted for each time point for each strain. Average, standard deviations (s.d.), *P*-values and statistical significance (Tables S1 and S2) were calculated using GraphPad Prism 6.0 software. Data shown in Fig. 1B and Fig. 4C were analysed by unpaired *t*-test, data shown in Fig. 1C-F were analysed by two-way ANOVA Tukey's multiple comparisons test, data shown in Fig. 4B were analysed by ordinary one-way ANOVA Dunnett's multiple comparisons test. Flow cytometric DNA quantification was performed according to Fraschini et al. (2001) on a Becton-Dickinson FACScalibur. Densitometric analysis of western blots was performed with ImageJ software.

Acknowledgements

We are grateful to Tim Huffaker, Daniel J. Lew, David Morgan, Simonetta Piatti, Elmar Schiebel and Jeremy Thorner for strains and antibodies. Some data in this paper forms part of Erica Raspelli's PhD thesis from the University of Milano Bicocca, 2013.

Competing interests

The authors declare no competing or financial interests.

Author contributions

Conceptualization: E.R., S.F., R.F.; Methodology: E.R., R.F.; Software: R.F.; Validation: E.R.; Formal analysis: E.R.; Investigation: E.R., S.F., R.F.; Data curation: E.R., R.F.; Writing - original draft: R.F.; Writing - review & editing: E.R., S.F.; Supervision: R.F.; Project administration: R.F.; Funding acquisition: R.F.

Funding

This work was supported by grants from Progetti di Ricerca di Interesse Nazionale (PRIN) and from the University of Milano Bicocca (FA) to R.F. E.R. is funded by a fellowship from the Associazione Italiana per Ricerca sul Cancro (AIRC), Love Design Rif:18196.

Supplementary information

Supplementary information available online at
http://jcs.biologists.org/lookup/doi/10.1242/jcs.213520.supplemental

References

Asano, S., Park, J.-E., Sakchaisri, K., Yu, L.-R., Song, S., Supavilai, P., Veenstra, T. D. and Lee, K. S. (2005). Concerted mechanism of Swe1/Wee1 regulation by multiple kinases in budding yeast. *EMBO J.* **24**, 2194-2204.

Berlin, V., Styles, C. A. and Fink, G. R. (1990). BIK1, a protein required for microtubule function during mating and mitosis in *Saccharomyces cerevisiae*, colocalizes with tubulin. *J. Cell Biol.* **111**, 2573-2586.

Bieling, P., Kandels-Lewis, S., Telley, I. A., van Dijk, J., Janke, C. and Surrey, T. (2008). CLIP-170 tracks growing microtubule ends by dynamically recognizing composite EB1/tubulin-binding sites. *J. Cell Biol.* **183**, 1223-1233.

Bodenmiller, B. and Aebersold, R. (2010). Quantitative analysis of protein phosphorylation on a system-wide scale by mass spectrometry-based proteomics. *Methods Enzymol.* **470**, 317-334.

Booher, R. N., Deshaies, R. J. and Kirschner, M. W. (1993). Properties of *Saccharomyces cerevisiae* wee1 and its differential regulation of p34CDC28 in response to G1 and G2 cyclins. *EMBO J.* **12**, 3417-3426.

Carvalho, P., Tirnauer, J. S. and Pellman, D. (2003). Surfing on microtubule ends. *Trends Cell Biol.* **13**, 229-237.

Carvalho, P., Gupta, M. L., Jr, Hoyt, M. A. and Pellman, D. (2004). Cell cycle control of kinesin-mediated transport of Bik1 (CLIP-170) regulates microtubule stability and dynein activation. *Dev. Cell* **6**, 815-829.

Cassani, C., Raspelli, E., Chiroli, E. and Fraschini, R. (2014). Vhs2 is a novel regulator of septin dynamics in budding yeast. *Cell Cycle* **13**, 1590-1601.

Fraschini, R. (2017). Fluorescence microscopy applied to the analysis of mitotic spindle dynamics. *Microscopy Book Series* **7**, 159-166.

Fraschini, R., Beretta, A., Sironi, L., Musacchio, A., Lucchini, G. and Piatti, S. (2001). Bub3 interaction with Mad2, Mad3 and Cdc20 is mediated by WD40 repeats and does not require intact kinetochores. *EMBO J.* **20**, 6648-6659.

Fraschini, R., Venturetti, M., Chiroli, E. and Piatti, S. (2008). The spindle position checkpoint: how to deal with spindle misalignment during asymmetric cell division in budding yeast. *Biochem. Soc. Trans.* **36**, 416-420.

Gladfelter, A. S., Kozubowski, L., Zyla, T. R. and Lew, D. J. (2005). Interplay between septin organization, cell cycle and cell shape in yeast. *J. Cell Sci.* **118**, 1617-1628.

Harvey, S. L. and Kellogg, D. R. (2003). Conservation of mechanisms controlling entry into mitosis: budding yeast wee1 delays entry into mitosis and is required for cell size control. *Curr. Biol.* **13**, 264-275.

Harvey, S. L., Charlet, A., Haas, W., Gygi, S. P. and Kellogg, D. R. (2005). Cdk1-dependent regulation of the mitotic inhibitor Wee1. *Cell* **122**, 407-420.

Heil-Chapdelaine, R. A., Oberle, J. R. and Cooper, J. A. (2000). The cortical protein Num1p is essential for dynein-dependent interactions of microtubules with the cortex. *J. Cell Biol.* **151**, 1337-1344.

Hotz, M., Leisner, C., Chen, D., Manatschal, C., Wegleiter, T., Ouellet, J., Lindstrom, D., Gottschling, D. E., Vogel, J. and Barral, Y. (2012). Spindle pole bodies exploit the mitotic exit network in metaphase to drive their age-dependent segregation. *Cell* **148**, 958-972.

Howell, A. S. and Lew, D. J. (2012). Morphogenesis and the cell cycle. *Genetics* **190**, 51-77.

Huffaker, T. C., Thomas, J. H. and Botstein, D. (1988). Diverse effects of beta-tubulin mutations on microtubule formation and function. *J. Cell Biol.* **106**, 1997-2010.

Jorgensen, P., Nishikawa, J. L., Breitkreutz, B. J. and Tyers, M. (2002). Systematic identification of pathways that couple cell growth and division in yeast. *Science* **297**, 395-400.

Keaton, M. A. and Lew, D. J. (2006). Eavesdropping on the cytoskeleton: progress and controversy in the yeast morphogenesis checkpoint. *Curr. Opin. Microbiol.* **9**, 540-546.

Keaton, M. A., Szkotnicki, L., Marquitz, A. R., Harrison, J., Zyla, T. R. and Lew, D. J. (2008). Nucleocytoplasmic trafficking of G2/M regulators in yeast. *Mol. Biol. Cell* **19**, 4006-4018.

Kellogg, D. R. (2003). Wee1-dependent mechanisms required for coordination of cell growth and cell division. *J. Cell Sci.* **116**, 4883-4890.

La Valle, R. and Wittenberg, C. (2001). A role for the Swe1 checkpoint kinase during filamentous growth of Saccharomyces cerevisiae. *Genetics* **158**, 549-562.

Lee, L., Tirnauer, J. S., Li, J., Schuyler, S. C., Liu, J. Y. and Pellman, D. (2000). Positioning of the mitotic spindle by a cortical-microtubule capture mechanism. *Science* **287**, 2260-2262.

Lengefeld, J., Hotz, M., Rollins, M., Baetz, K. and Barral, Y. (2017). Budding yeast Wee1 distinguishes spindle pole bodies to guide their pattern of age-dependent segregation. *Nat. Cell Biol.* **19**, 941-951.
Lew, D. J. (2003). The morphogenesis checkpoint: how yeast cells watch their figures. *Curr. Opin. Cell Biol.* **15**, 648-653.
Lianga, N., Williams, E. C., Kennedy, E. K., Doré, C., Pilon, S., Girard, S. L., Deneault, J.-S. and Rudner, A. D. (2013). A Wee1 checkpoint inhibits anaphase onset. *J. Cell Biol.* **201**, 843-862.
Lobjois, V., Jullien, D., Bouché, J.-P. and Ducommun, B. (2009). The polo-like kinase 1 regulates CDC25B-dependent mitosis entry. *Biochim. Biophys. Acta* **1793**, 462-468.
Lobjois, V., Froment, C., Braud, E., Grimal, F., Burlet-Schiltz, O., Ducommun, B. and Bouche, J. P. (2011). Study of the docking-dependent PLK1 phosphorylation of the CDC25B phosphatase. *Biochem. Biophys. Res. Commun.* **410**, 87-90.
Longtine, M. S., Theesfeld, C. L., McMillan, J. N., Weaver, E., Pringle, J. R. and Lew, D. J. (2000). Septin-dependent assembly of a cell cycle-regulatory module in Saccharomyces cerevisiae. *Mol. Cell. Biol.* **20**, 4049-4061.
Mahajan, K., Fang, B., Koomen, J. M. and Mahajan, N. P. (2012). H2B Tyr37 phosphorylation suppresses expression of replication-dependent core histone genes. *Nat. Struct. Mol. Biol.* **19**, 930-937.
Makrantoni, V., Corbishley, S. J., Rachidi, N., Morrice, N. A., Robinson, D. A. and Stark, M. J. (2014). Phosphorylation of Sli15 by Ipl1 is important for proper CPC localization and chromosome stability in Saccharomyces cerevisiae. *PLoS ONE* **9**, e89399.
Maniatis, T., Fritsch, E. F. and Sambrook, J. (1992). *Molecular Cloning: A Laboratory Manual*. NY: Cold Spring Harbor Laboratory Press, Cold Spring Harbor Laboratory.
McMillan, J. N., Sia, R. A. L., Bardes, E. S. G. and Lew, D. J. (1999). Phosphorylation-independent inhibition of Cdc28p by the tyrosine kinase Swe1p in the morphogenesis checkpoint. *Mol. Cell. Biol.* **19**, 5981-5990.
Michael, W. M. and Newport, J. (1998). Coupling of mitosis to the completion of S phase through Cdc34-mediated degradation of Wee1. *Science* **282**, 1886-1889.
Moore, J. K., D'Silva, S. and Miller, R. K. (2006). The CLIP-170 homologue Bik1p promotes the phosphorylation and asymmetric localization of Kar9p. *Mol. Biol. Cell* **17**, 178-191.
Morgan, D. O. (1997). Cyclin-dependent kinases: engines, clocks, and microprocessors. *Annu. Rev. Cell Dev. Biol.* **13**, 261-291.
Nakajima, Y., Cormier, A., Tyers, R. G., Pigula, A., Peng, Y., Drubin, D. G. and Barnes, G. (2011). Ipl1/Aurora-dependent phosphorylation of Sli15/INCENP regulates CPC-spindle interaction to ensure proper microtubule dynamics. *J. Cell Biol.* **194**, 137-153.
Pal, G., Paraz, M. T. Z. and Kellogg, D. R. (2008). Regulation of Mih1/Cdc25 by protein phosphatase 2A and casein kinase 1. *J. Cell Biol.* **180**, 931-945.
Park, C. J., Park, J.-E., Karpova, T. S., Soung, N.-K., Yu, L.-R., Song, S., Lee, K. H., Xia, X., Kang, E., Dabanoglu, I. et al. (2008). Requirement for the budding yeast polo kinase Cdc5 in proper microtubule growth and dynamics. *Eukaryot. Cell* **7**, 444-453.
Pearson, C. G. and Bloom, K. (2004). Dynamic microtubules lead the way for spindle positioning. *Nat. Rev. Mol. Cell Biol.* **5**, 481-492.
Piatti, S., Venturetti, M., Chiroli, E. and Fraschini, R. (2006). The spindle position checkpoint in budding yeast: the motherly care of MEN. *Cell Div.* **1**, 2.
Raspelli, E., Cassani, C., Lucchini, G. and Fraschini, R. (2011). Budding yeast Dma1 and Dma2 participate in regulation of Swe1 levels and localization. *Mol. Biol. Cell* **22**, 2185-2197.
Raspelli, E., Cassani, C., Chiroli, E. and Fraschini, R. (2015). Budding yeast Swe1 is involved in the control of mitotic spindle elongation and is regulated by Cdc14 phosphatase during mitosis. *J. Biol. Chem.* **290**, 1-12.
Rudner, A. D. and Murray, A. W. (2000). Phosphorylation by Cdc28 activates the Cdc20-dependent activity of the anaphase-promoting complex. *J. Cell Biol.* **149**, 1377-1390.
Rudner, A. D., Hardwick, K. G. and Murray, A. W. (2000). Cdc28 activates exit from mitosis in budding yeast. *J. Cell Biol.* **149**, 1361-1376.
Russell, P., Moreno, S. and Reed, S. I. (1989). Conservation of mitotic controls in fission and budding yeasts. *Cell* **57**, 295-303.
Sakchaisri, K., Asano, S., Yu, L.-R., Shulewitz, M. J., Park, C. J., Park, J.-E., Cho, Y.-W., Veenstra, T. D., Thorner, J. and Lee, K. S. (2004). Coupling morphogenesis to mitotic entry. *Proc. Natl. Acad. Sci. USA* **101**, 4124-4129.
Schindelin, J., Arganda-Carreras, I., Frise, E., Kaynig, V., Longair, M., Pietzsch, T., Preibisch, S., Rueden, C., Saalfeld, S. et al. (2012). Fiji: an open-source platform for biological-image analysis. *Nat. Methods* **9**, 676-682.
Sherman, F. (1991). Getting started with yeast. *Methods Enzymol.* **194**, 3-21.
Simpson-Lavy, K. J., Zenvirth, D. and Brandeis, M. (2015). Phosphorylation and dephosphorylation regulate APC/C(Cdh1) substrate degradation. *Cell Cycle* **14**, 3138-3145.
Snead, J. L., Sullivan, M., Lowery, D. M., Cohen, M. S., Zhang, C., Randle, D. H., Taunton, J., Yaffe, M. B., Morgan, D. O. and Shokat, K. M. (2007). A coupled chemical-genetic and bioinformatic approach to Polo-like kinase pathway exploration. *Chem. Biol.* **14**, 1261-1272.
Song, S. and Lee, K. S. (2001). A novel function of Saccharomyces cerevisiae CDC5 in cytokinesis. *J. Cell Biol.* **152**, 451-469.
Sorger, P. K. and Murray, A. W. (1992). S-phase feedback control in budding yeast independent of tyrosine phosphorylation of p34cdc28. *Nature* **355**, 365-368.
Stegmeier, F., Visintin, R. and Amon, A. (2002). Separase, polo kinase, the kinetochore protein Slk19, and Spo12 function in a network that controls Cdc14 localization during early anaphase. *Cell* **108**, 207-220.
Tirnauer, J. S., O'Toole, E., Berrueta, L., Bierer, B. E. and Pellman, D. (1999). Yeast Bim1p promotes the G1-specific dynamics of microtubules. *J. Cell Biol.* **145**, 993-1007.
van de Weerdt, B. C. M. and Medema, R. H. (2006). Polo-like kinases: a team in control of the division. *Cell Cycle* **5**, 853-864.
Wach, A., Brachat, A., Pöhlmann, R. and Philippsen, P. (1994). New heterologous modules for classical or PCR-based gene disruptions in *Saccharomyces cerevisiae*. *Yeast* **10**, 1793-1808.
Woodruff, J. B., Drubin, D. G. and Barnes, G. (2010). Mitotic spindle disassembly occurs via distinct subprocesses driven by the anaphase-promoting complex, Aurora B kinase, and kinesin-8. *J. Cell Biol.* **191**, 795-808.
Yeh, E., Skibbens, R. V., Cheng, J. W., Salmon, E. D. and Bloom, K. (1995). Spindle dynamics and cell cycle regulation of dynein in the budding yeast, *Saccharomyces cerevisiae*. *J. Cell Biol.* **130**, 687-700.